

THE ROLE OF INTERPHASE BOUNDARIES IN THE DEFORMATION
BEHAVIOUR OF FINE-GRAINED Sn–38wt.%Pb EUTECTICS

F. Muktepavela, G. Bakradze, R. Zabels

Institute of Solid State Physics, University of Latvia
8 Kengaraga Str., Riga, LV-1063, LATVIA

The mechanical properties of binary Sn–38wt.%Pb eutectic alloys in the deformed and annealed states were investigated at room temperature using tensile, micro- and nano-indentation tests. The softening and high plasticity of a deformed Sn–Pb eutectic are explained as a result of grain boundary sliding (GBS) and fast diffusion-driven processes developing along the Sn–Pb interphase boundaries (IBs). From the results of micro- and nano-hardness measurements it follows that the Sn and Pb phases in the annealed eutectic are strengthened, and the relaxation processes occur mainly at the IB. Such IBs in the annealed Sn–Pb eutectic act as barriers to the motion of a dislocation ensemble when the size of the plastic zone is comparable with the grain size, lowering the hardness values due to the development of GBS when more grains are involved in the process of deformation. The nanohardness and elastic modulus values obtained evidence that an IB in the Sn–Pb eutectic is to be considered as a separate phase with its own mechanical properties.

Key words: *Sn–38wt.%Pb eutectic, interphase boundary energy, grain boundary sliding, microhardness, nanohardness.*

1. INTRODUCTION

Sn–Pb alloys are employed in many technical applications as components of antifriction alloys, as structural materials in the microelectronics industry, etc. In such applications the electrical, thermal and mechanical properties of the Sn–Pb alloys are essential. Lately, considerable interest in the mechanical behaviour of Sn–Pb alloys has also arisen from the standpoint of renovating or replacing the aged pipes in church organs [1]. Nearly eutectic Sn–Pb alloys have long been a common material for organ pipes produced by the extrusion process. The Sn–38wt.%Pb alloy, which exhibits structural superplasticity, allows the initial material to be severely deformed without losing its integrity in the extrusion process at a macroscopic level.

As was shown previously [2-4], the structural superplasticity of Sn–Pb eutectics is generally attributed to the grain boundary sliding (GBS) mechanism. However, localization of the plastic deformation during GBS can result in different structural and phase transitions. First of all, GBS inevitably leads to the formation of micropores/microcracks at the grain boundaries (GBs). The process of crack opening/closing strongly depends on the work of adhesion W_a or, alternatively, on the gain in the free energy ΔF after the new interface has been formed. Its value is defined as

$$\Delta F = \gamma_s^A + \gamma_s^B - \gamma_{ib}^{AB}, \quad (1)$$

where γ_s^A, γ_s^B are the surface energies of materials A and B , respectively;
 γ_{ib}^{AB} is the energy of the interphase boundary (IB) between materials A and B .

It is obvious that the IB energy is an integral characteristic of physical and chemical properties of a particular boundary and, therefore, can affect the development of the accommodation processes during GBS.

In [5, 6] we have shown that in eutectics with high IB energy (such as Al–Sn, Zn–Sn) GBS occurs predominantly by dislocation glide followed by a marked strengthening of the IB region. However, in the superplastic Sn–Pb and Cd–Sn eutectics with low IB energy values the GBS process is accompanied by diffusion-driven accommodation processes with closing the micropores/microcracks [5, 6].

Previously, quantitative estimations of the healing rate of micropores/microcracks in Sn–Pb under the action of capillary forces (that could be done by Eq. (1)) were absent. Accordingly, the interpretation of the results obtained in [5, 6] was not quite correct. Another experimental problem that remained then unsolved was the distinguishing between the mechanical properties of separate phases and those of IBs in the Sn–Pb eutectic. At that time this was mainly connected with experimental difficulties at the investigation into mechanical properties of the phases and IB in such a fine-grained material as the Sn–Pb eutectic. Currently, the micro-indentation tests (using low loads) along with nanoindentation ones (using ultra-low loads) allow such measurements to be performed (see Sect. 2).

In the present contribution, both the methods of microhardness and nano-hardness have been used to investigate the mechanical properties of Sn and Pb phases and the role of IB in the deformation process of Sn–Pb eutectic alloy. The results of tensile tests have been analysed and the time needed for micropore/microcrack closing under the influence of capillary forces on the IBs in the Sn–Pb eutectic has been estimated.

2. EXPERIMENTAL

The Sn–38wt.%Pb eutectic alloy was prepared from highly pure Sn and Pb metals. The ingots of the eutectic were annealed and deformed by compression ($\varepsilon = 80\%$) at 300 K. The bulk mechanical properties of the alloy were investigated using standard machines for tensile strength tests. Bimetallic solid phase joints (Sn/Pb) with atomically clean interfaces were obtained by a special method of cold welding at room temperature (RT) [6] and used as a macromodel of the deformed IB. The strength properties of the joints were determined by the shear test. The hardness measurements in bulk of the eutectic alloy were carried out using a standard Brinell tester ($P = 5$ kg).

The local hardness of individual grains and the development of GBS were studied using micro- and nanoindentation testers. Indentation tests are probably the most common tools applied to characterize the mechanical properties of polycrystalline materials. One of the advantages of these methods is the possibility to investigate the deformation behaviour of a particular material in a wide range of the deformation volumes. This can be achieved using different loads for testing. On the one hand, the use of low loads in the indentation experiments allows determination of the mechanical properties inside a grain. On the other, using higher loads it is possible to observe the collective processes when several grains

are involved into deformation; for example, under certain conditions the GBS contribution to the total deformation process could be revealed.

The microhardness tests were performed using a square-based Vickers pyramid as the indenter. A modified PMT-3 (LOMO) microhardness tester with a precise loading device and vibration damping allowed accurate measurements to be performed using loads in the range of 1.4–500 mN. A typical accuracy of the imprint diagonal (d_{impr}) measurements was 3–7%. The indentation depth for the Vickers indenter at each load was determined as $h = d_{impr}/7$. The main results have been presented in the form of microhardness dependence $H = f(h)$. The nano-hardness and elastic modulus were determined by an MTS G200 nanoindenter using a Berkovich diamond tip ($R < 20$ nm) and the depth-sensing dynamic indentation technique (strain rate 0.05 s⁻¹, maximum indentation depth 1600 nm). The hardness and Young's modulus as functions of the indenter displacement were measured automatically, using the loading-unloading curve. The force–displacement data were interpreted using the MTS TestWorks 4 software.

The investigations into the structure around the imprints were carried out with the help of optical (Eclipse L150) and electron (SEM with X-ray spectral analysis JSM-5300) microscopes. All experiments were performed at room temperature.

3. RESULTS AND DISCUSSION

3.1. Bulk mechanical properties and estimation of the pore closing time

Table 1 demonstrates the results of mechanical tests of the Sn–Pb eutectic and bimetallic Sn/Pb joints in the annealed and deformed (total deformation $\varepsilon = 80\%$) states. The deformation-induced softening ($\Delta H/H$, %) is one of the main parameters that characterize the superplastic state of material, being defined as a relative decrease in the Brinell hardness of the alloy after deformation:

$$\Delta H/H = \frac{H_a - H_d}{H_a} 100\%,$$

where H_a and H_d are the hardness values of the eutectic in the annealed and deformed states, respectively.

As apparent from Table 1, in the deformed state both the Sn–Pb alloy and the Sn/Pb joint are more plastic than in the annealed state, both of them exhibiting a considerable mechanical softening ($\Delta H/H = 65\%$). As known, plastic deformation usually causes hardening of the material under deformation. In the case under consideration it does not occur. This peculiarity of the deformation behaviour most probably can be attributed to the properties of the IB in a Sn–Pb system. In [5] we have shown that the alloy deformation occurs at the IB between Sn and Pb in the form of superplastic GBS. As the room temperature for the Sn–Pb eutectics exceeds half of its melting point, T_m , the development of GB diffusion is facilitated at this temperature. Thus, there are possible fast processes of the contact restoration between the two phases owing to the free energy gain (see Eq. (1) and the data of Table 1 for the surface and IB energies).

Table 1

Strength σ of Sn–Pb eutectic and Sn/Pb bimetallic joint, softening parameter $\Delta H/H$ of Sn–Pb eutectic, and surface (γ^{Pb_s} , γ^{Sn_s}) and interphase boundary (γ_{ib}) energies [6, 7]

Properties Material	σ [MPa] and fracture mode at 293 K				$\Delta H/H$, %	γ_{ib} , J/m ²	$\gamma_{s_2}^{Pb}$ J/m ²	$\gamma_{s_2}^{Sn}$ J/m ²
	annealed state		deformed state					
Sn–Pb eutectic	35	ductile	25	superplastic	65	0.07	0.56	0.67
Sn/Pb joint	20	ductile, inside Pb	15	superplastic, along the Sn–Pb interface [5]				

We will now estimate the time needed to restore the contact between the Sn and Pb phases. This process can also be treated as the micropore/microcrack closing under the action of capillary forces at high homologous temperatures. As shown in [8, 9], the sintering time τ of a fine pore with the average size d_p under the action of capillary force is

$$\tau \approx k \cdot T \cdot d_p^2 / D_{ib} \cdot a^2 \cdot W_a, \quad (2)$$

where a is the interatomic spacing,

k is the Boltzmann constant,

D_{ib} is the diffusion coefficient of grain boundary,

W_a is the adhesion work.

The diffusion transport taking place directly along the IB was investigated earlier [6]. The estimation made in this work has given very high values of the diffusion coefficient ($D_{ib} \sim 10^{-10}$ – 10^{-11} m²/s) obtained in the range of 0.4–0.6 T_m . If we took typical values for the Sn–Pb system: $D_{ib} \sim 10^{-11}$ m²/s [6], $d_p \approx 1$ μ m, (d_p/a) $\approx 5 \cdot 10^3$, $W_a \approx 1$ J/m², $T = 300$ K, the values obtained for the sintering time would be of the order of $\tau \approx 0.01$ s.

Summing up this data it is possible to conclude that the diffusion processes occur actively in the Sn–Pb alloy during plastic deformation even at RT, inducing the pore closing and the restoration of the interphase contact during GBS. These processes are the reason for the softening of the Sn/Pb IB during plastic tensile/compression deformation.

3.2. Microhardness

In this subsection we will consider the microhardness test results of the Sn–Pb alloy in the annealed and deformed (total deformation $\varepsilon = 80\%$) states. As is seen from Fig. 1, the microhardness values for the deformed Sn–Pb alloy are lower in comparison with those for the annealed one, which is in agreement with the deformation-induced softening effect discussed above. The microhardness values of the annealed and deformed alloy depend on the indentation depth.

A noticeable decrease in the microhardness was observed for Sn–Pb eutectic in the deformed state in the region of small depths ($h < 3$ μ m) when the imprint size is comparable with the grain size of the alloy. The decrease in the microhardness can first of all be explained by poor connection between the top and adjacent grains; this, in turn, causes a more efficient GBS (the superplastic state of GB). Another explanation could be related to the intensive deformation-induced

processes of mass transfer (diffusion) on the free surface of grains. This result complies with the data of Table 1 and confirms the deformation softening at the interface.

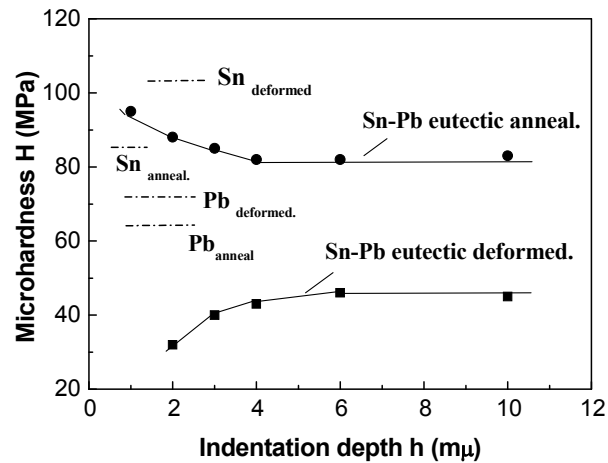


Fig. 1. The microhardness-indentation depth curves for Sn-Pb eutectic alloy in the deformed and annealed states. The microhardness levels for Sn and Pb in the annealed and deformed states are indicated.

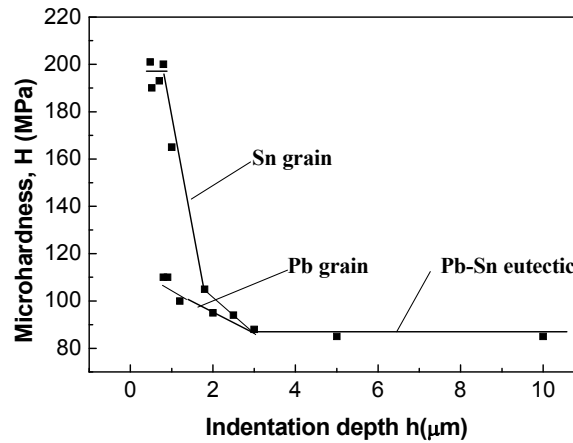


Fig. 2. The microhardness-indentation depth curve for the annealed Sn-Pb eutectic alloy showing the microhardness values in separate Sn and Pb phases.

It is of interest to analyze the microhardness data of the annealed Sn-Pb eutectic. At higher depths the microhardness values do not depend on the load and are at a level of $H \approx 80-84$ MPa. The increase in the microhardness of the annealed alloy in the near-surface layers ($h < 3 \mu m$) is most likely to be connected with the internal testing of the phase. To confirm this assumption, an experiment employing lower loads was performed. As can be seen from Fig. 2, the use of low loads (0.12–0.14 g) has allowed imprints to be put right at the centre of the tin and lead separate phases (see Fig.3a) and thus their microhardness to be determined. The microhardness values of the Sn phase are higher than those of the Pb phase, which is natural. It is necessary to point out that, even at the use of very small loads (0.12 g)

for the indentation inside a Pb grain, the plastic zone created by the imprint inevitably involves the IB into the deformation process (Fig. 3a). However, the obtained microhardness values (at $h = 0.5 \mu\text{m}$) both for Sn ($H = 200 \text{ MPa}$) and Pb ($H = 110 \text{ MPa}$) grains are very high in comparison with such values for the Sn and Pb original materials. This comparison with the initially pure components is not absolutely correct; despite the fact that the RT solubility of lead in tin is insignificant (less than 0.2 at.%) while such solubility of tin in lead can reach 2 at.%, this does not noticeably affect the microhardness values ($<10 \text{ MPa}$). At higher loads ($>0.5\text{--}1 \text{ g}$) when many grains are involved in the deformation process (Fig. 3b), one could estimate the microhardness of the Sn–Pb eutectic using a simple additive rule – the mixture law:

$$H_{\text{Pb-Sn}} = 0.62 \cdot H_{\text{Sn}} + 0.38 \cdot H_{\text{Pb}}. \quad (3)$$

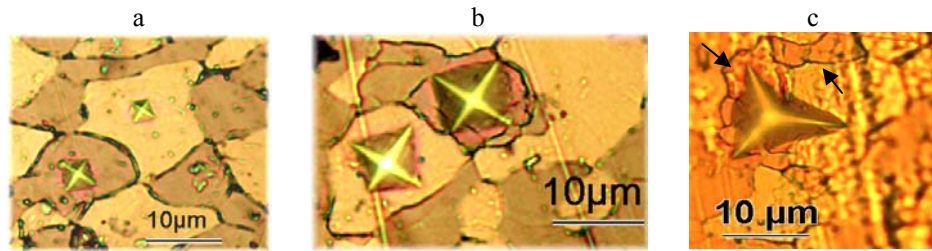


Fig. 3. The micrographs of the imprints made using the loads: $P = 1.4 \text{ mN}$ (a), $P = 5 \text{ mN}$ (b) in the Sn phase (bright grains) and Pb phase (darker grains), $P = 7 \text{ mN}$ (c); (a), (b) refer to the indentation made by Vickers' indenter (microindentation), and (c) represents the imprint made by Berkovich's indenter (nanoindentation). The outlined traces of GBS are indicated by arrows.

Taking the microhardness data (at high loads) for the annealed Sn ($H_{\text{Sn}} = 84 \text{ MPa}$) and Pb ($H_{\text{Pb}} = 66 \text{ MPa}$), we obtain the $H_{\text{Pb-Sn}}$ value equal to 77 MPa . At the same time, these data measured in the central part of phases at $h = 0.5 \mu\text{m}$ (see above) give the value of 165 MPa . Both the values do not agree with the experimentally obtained ($82\text{--}85 \text{ MPa}$). This means that it is not quite correct to consider the Sn–Pb eutectic as a mechanical mixture of two phases – such eutectic should rather be treated as a three-phase alloy with the IB having its own mechanical properties.

The microhardness-indentation depth dependence has been shown for grains of both the phases, Pb and Sn. The microhardness values increase when the indentation depth decreases (i.e. at low loads). This phenomenon is known as the indentation size effect (ISE) for single crystals described by the law: $H = c \cdot h^{-m}$, where c is a constant [10, 11]. For Pb and Sn single crystals the power m is 0.14 and 0.16, respectively.

We will assume the grains of the phases to be single crystals. The exponential law is observed with the power $m = 0.17$ for the Pb phase. It is interesting that on the curve of Sn phase in Fig. 2 there are three flex points. For its top portion (in the range $h = 0.5\text{--}1.8 \mu\text{m}$) $m = 0.5$ is valid, while for the bottom portion ($h = 1.8\text{--}3 \mu\text{m}$) $m = 0.12$. This implies the influence of different factors during the indentation. These m values are too high for Pb and Sn, hence, the size factor is not the reason for the change of hardness in this range of depths. A similar conclusion

was drawn in the paper describing nanoindentation measurements in the Sn–Pb eutectic [12]. The authors show that the hardness decreases with the indentation depth increasing owing to creep (i.e. thermally activated diffusion) processes. Unfortunately, the authors have used the hardness data referring to both phases, without distinguishing between the properties of separate phases and those of IBs themselves. At the same time, the value $m = 0.5$ obtained for Sn phase in the range $h = 0.5\text{--}1.8\ \mu\text{m}$ is usually the exponent in Hall–Petch’s law for polycrystalline materials:

$$H = H_0 + k \cdot d^{-0.5}, \quad (4)$$

where H is the hardness at a given load;
 H_0 is the hardness inside a grain (or of a single crystal);
 k is a constant;
 d is the grain size.

It is possible to suggest that the IB acts as a barrier to the development of a plastic zone around the imprint. The schematic picture of the formation of a plastic zone during indentation is shown in Fig. 4. This zone’s size is $2 \cdot r = f \cdot d_{impr}$, where $f > 1$ is a coefficient [13]. In [14] the f values for polycrystalline Zn were estimated to be in the range 2.8–3. As seen from Fig. 3, inside the Sn phase the minimum imprint size is $d_{impr} = 3.5\ \mu\text{m}$ ($H = 200\ \text{MPa}$ at $h = 0.5\ \mu\text{m}$); in this case the plastic zone is $2r = 10\ \mu\text{m}$, which is close to the average grain size. Thus, the IB can act as a barrier to the motion of a dislocation ensemble and to the spread of a plastic zone. If such a zone is spreading around the imprint beyond the grain limits, this would lead to the interaction of the dislocation ensemble with the IB and to the deformation-induced GBS, as can be seen in Fig. 3*b*. A similar result has been obtained in the work devoted to the development of GBS in Zn during micro-indentation [14].

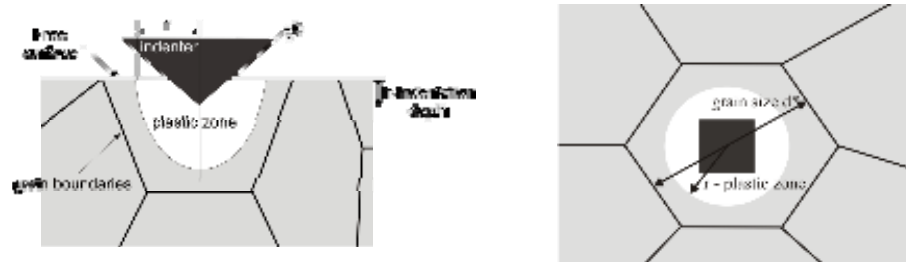


Fig. 4. The scheme of plastic zone formation during indentation. The plastic zone size is assumed to be a hemisphere with radius r .

Thus, GBS can be activated by piling-up the dislocation ensembles at the IB, which leads to relaxation of the stresses, facilitating the plastic deformation and decreasing the microhardness values at higher indentation depths.

3.3. Nanohardness and elastic modulus

Since the microhardness tester used in this work has restriction in the range of low loads, we could not observe the rise in hardness at the IB itself. To verify the validity of the assumption about the barrier action of interphase boundary, nanoindentation measurements using continuous loading (up to depths of 1–1.5 μm) have been made. The results evidence that there is a rise within depths

280–300 nm (see curves $H-h$ in Fig. 5a). For the Berkovich indenter the indentation depth was calculated as

$$h = \frac{a}{2\sqrt{3} \operatorname{tg} 65.3^\circ}, \quad (5)$$

where a is the side length of the imprint.

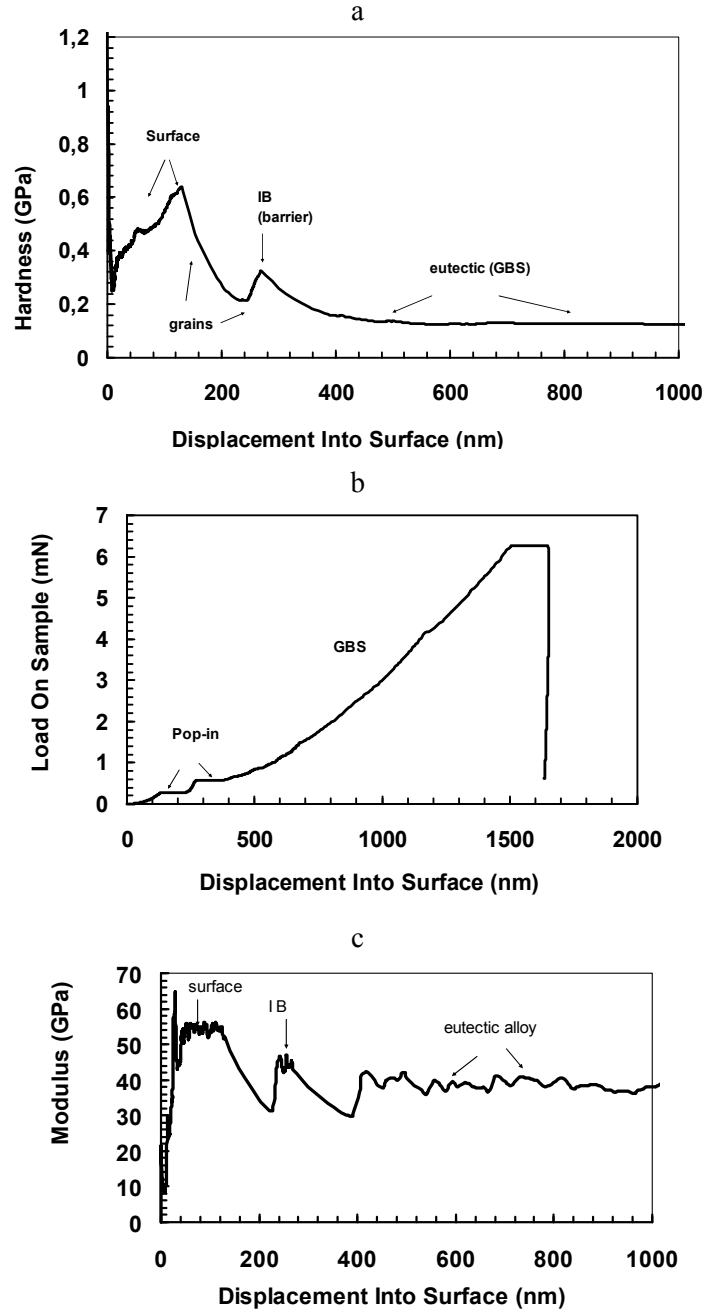


Fig. 5. The nanohardness (a), load (b) and modulus (c) vs. displacement for the annealed Sn–Pb eutectic alloy.

The size of a plastic zone in this case is $2 \cdot r = 6\text{--}7 \mu\text{m}$. As seen from Fig. 3c, the measurements of nanohardness were taken at the place where the average grain size was about $7\text{--}8 \mu\text{m}$. Here, the IB acts as a barrier to the plastic zone's spread induced by indentation. The IB hardening effect is 40–50%. A similar increase in the nanohardness near a GB was observed in Ni samples by Yang *et al.* [15], and in Mo samples by Eliash *et al.* [16]. This is in a good agreement with the results obtained by us in the microhardness test at $h = 500 \text{ nm}$, taking into account the difference in the used indenters – a Vicker's (microindentation) and a Berkovich's (nanoindentation) ones. The first portion of the curve ($h < 200 \text{ nm}$) could be interpreted as the ISE; however, factor m of the order of 0.24 revealed in the work is higher than is needed for the ISE in Pb and Sn phases. Similar to the case of the microhardness measurements, it is possible to suggest here the influence of creep processes, or, considering the very thin near-surface layers investigated, the influence of SnO_2 , whose hardness is very high ($\approx 10 \text{ GPa}$).

The decrease in the nanohardness values at high loads ($h > 300 \text{ nm}$) is attributed to the change in the plastic deformation mechanism: from the dislocation sliding inside a grain to the development of GBS as the basic mechanism of deformation influencing the hardness values (for microhardness values see Fig. 2). The micrograph in Fig. 3c shows the development of GBS around the imprint made by the Berkovich indenter at high load ($h \approx 1.5 \mu\text{m}$). The above mentioned processes of changes in the plastic deformation mechanism can also be seen in the curve showing continuous indenter displacement into the surface (Fig. 5b). The so-called “pop-in” phenomena are connected with the homogeneous nucleation and generation of dislocations [17].

The nanoindentation tests have allowed us to trace the changes in the elastic Young's modulus (E) at different stages of the indenter displacement (Fig. 5c). According to the mixture rule, the bulk modulus of Sn–Pb eutectic should be equal to 34 GPa (if there are taken usual values: $E_{\text{Sn}} = 42 \text{ GPa}$, $E_{\text{Pb}} = 14\text{--}16 \text{ GPa}$). The data obtained at a small indentation depth are very high ($E > 55 \text{ GPa}$) and possibly show the properties of a surface layer whose influence weakens at moving away from the surface. The sudden rise in E up to 45 GPa at $h = 280 \text{ nm}$ specifies the existence of another material, and probably corresponds to the elastic properties of the Sn/Pb interphase boundaries at the time of barrier action. At $h > 1 \mu\text{m}$ the elastic modulus $E = 38 \text{ GPa}$ corresponds well to that of the heterogeneous Sn–38%Pb eutectic alloy.

4. CONCLUSIONS

In the work we have shown that both the softening of the deformed Sn–Pb eutectic and the superplastic GBS on a severely deformed interface boundary are caused by fast developing sintering (micropore closing) processes under the action of capillary forces on the Sn–Pb IB. These processes are thermodynamically favourable owing to the low values of the interphase energy (0.07 J/m^2) and kinetically allowed due to the relatively high homologous temperature ($>0.5 \cdot T_m$).

With the help of micro- and nanohardness testers it has been shown that the phases in the annealed eutectic are strengthened and the relaxation processes occur

mainly on the interphase boundaries. These IBs can act as barriers to the motion of dislocation ensemble when the plastic zone size is comparable with that of a grain and can lower the hardness values because of the GBS development when more grains are involved in the process of deformation. GBS as a relaxation process removes the stresses at the IB, providing a further transfer of sliding along the IB and leading to the decrease in the microhardness. The obtained nanohardness and elastic modulus values evidence that the IB in the Sn–Pb eutectic has to be treated as a separate phase with its own mechanical properties.

The results obtained in the present work can be used for estimation of the operational stability of Sn–Pb alloys: the inevitably arising stress concentrators and even small cracks in such an alloy can be removed in the fast relaxation processes at RT. At the same time, under the conditions of local indentation the IBs can play the role of barriers to the development of plastic deformation.

ACNOWLEDGEMENTS

This work was financially supported by the project INTAS (05-1000008-8120) and Latvian Science Council (05.1705).

REFERENCES

1. Baretzky, B., Friesel, M., Petelin, A., Mazilkin, A., & Straumal, B. (2006). *Def. Diff. Forum*, 249, 275–280.
2. Padamanabhan, K.A., & Davies, J. (1980). *Superplasticity*. Berlin: Springer, 280.
3. Nabarro, F.R.N. (2002). *Metall. Mater. Trans. A*, 33, 213–230.
4. Kashyap, B.P., Arieli, A., & Mukherjee, A.K. (1985). *J. Mater. Sci.*, 20, 2661–2668.
5. Muktepavela, F., & Maniks, J. (2002). *J. Interf. Sci.*, 10, 21–26.
6. Muktepavela, F., & Maniks, J. (2003). *Def. Diff. Forum* 216–217, 169–174.
7. Missol, W. (1975). *Energia powierzchni rozdziału faz w metalach*. Katowice: Siack, 193.
8. Geguzin, Ya.E. (1967). *Physics of sintering*. Moscow: Nauka, 322. (in Russian).
9. Geguzin, Ya.E. (1976). *Dokladi Akademii Nauk*, 229, 601–603.
10. Varchenya, S.A., Muktepavel, F.O., & Upit, G.P. (1970). *Phys. Stat. Sol.*, A, (1) K165-7.
11. Nix, W.D., & Gao, H.J. (1998). *J. Mech. Phys. Sol.* 46, 411-418.
12. Gomez, J., & Basaran, G. (2006). *Intern. J. Sol. Struct.*, 43, 1505-1527.
13. Durst, K., Backes, S., & Goeken, M. (2005). *Scr. Met.*, 52, 1093-1098.
14. Muktepavela, F., Bakradze, G., & Sursaeva, V. (2008). *J. Mater. Sci.*, 43, 3848-3854.
15. Yang, B., & Vehoff, H. (2007). *Acta Mater.*, 55, 849-856.
16. Eliash, T., Kazakevich, M., Semenov, V.N., & Rabkin, E. (2008). *Acta Mater.*, 56, 5640–5652.
17. Goeken, M., & Kemp, M. (2001). *Z. Metallk.*, 92, 1061–1066.

STARPFĀŽU ROBEŽU LOMA SMALKGRAUDAINĀS Sn–38at.%Pb EITEKTIKAS PLASTISKĀ DEFORMĀCIJĀ

F. Muktepāvela, G. Bakradze, R. Zabels

Kopsavilkums

Sn–Pb eitektiskais sakausējums tiek plaši pielietots gan elektrotehnikā, gan arī aparātībūvē. Darbā veikti deformētas un atkvēlinātas binārās Sn–38wt.%Pb

eitektikas mehānisko īpašību un struktūras pētījumi, izmantojot stiepes, mikro- un nanocietības metodes. Deformētas eitektikas augstais plastiskums un mīkstināšanās deformācijas procesā izskaidroti ar slīdēšanu un difūzijas kontrolētu relaksācijas procesu norisi pa starpfāžu robežām. Atkvēlinātā eitektikā Pb un Sn fāzes uzrāda relatīvi augstu stiprību, bet deformācijas procesi ir lokalizēti starpfāžu robežās. Nanocietības un Junga moduļa dati liecina par to, ka starpfāžu robežas var uzskatīt par trešo fāzi, kurai ir savas īpašības, kas nosaka eitektikas plastiskumu.

23.01.2009.